



Diffusion Weighted (DW) MRI in Correlation with Dynamic Contrast Enhanced MRI for Characterization of Ovarian Masses

Doaa Abbas Radwan ^{a*}, Fatma Anas Elshaarawy ^a, Omnia Abd Elfattah Gad ^b and Aly Aly Elbarbary ^a

^a Radio-diagnosis and Medical Imaging Department, Faculty of Medicine, Tanta University, Egypt.

^b Clinical Oncology and Nuclear Medicine Department, Faculty of Medicine, Tanta University, Egypt.

Authors' contributions

This work was carried out in collaboration among all authors. All authors read and approved the final manuscript.

Article Information

DOI: 10.9734/JAMMR/2022/v34i1931431

Open Peer Review History:

This journal follows the Advanced Open Peer Review policy. Identity of the Reviewers, Editor(s) and additional Reviewers, peer review comments, different versions of the manuscript, comments of the editors, etc are available here: <https://www.sdiarticle5.com/review-history/84922>

Original Research Article

Received 20 January 2022

Accepted 30 March 2022

Published 06 June 2022

ABSTRACT

Background: Ovarian tumors; are the second most common gynecological tumor and in women are the fifth commonest tumor. Preoperative differentiation between benign and malignant tumors is essential to decide whether surgery is required, and which type of surgery is appropriate avoiding unnecessary surgery. In addition to conventional imaging, dynamic contrast and diffusion weighted images can aid in the separation of benign from malignant ovarian tumors. DWI is based on the notion that water molecules can freely diffuse in a low-cellular environment, but tissue hypercellularity restricts this. As a result, unlike most benign tumors, malignant ovarian tumors have restricted diffusion due to their hypercellular structure. DCE-MRI depends on contrast agent leaking from capillaries into extravascular extracellular space to allow for quantitative ovarian lesions characterisation.

Aim of the Work: To evaluate the role of diffusion- weighted MR imaging correlated to dynamic contrast enhanced MRI in characterization of ovarian masses.

Patients and Methods: thirty female patients were included in this study. Who referred to the radiology department by ovarian masses. All patients underwent detailed history taking, laboratory investigations, Pelvic ultrasound examination and MRI examination with DWI and DCE MRI. The correlation was done between MRI findings and the final pathological diagnosis.

*Corresponding author;

Results: The sensitivity of conventional MRI was 72.73% while that of DWI was 100%. The specificity was lower for DWI (57.89%) compared to conventional MRI (73.68%), The mean ADC values for malignant lesions were $(0.91 \times 10^{-3} \pm 0.25 \text{ SD mm}^2/\text{s})$, while that for benign lesions were $(1.68 \times 10^{-3} \pm 0.65 \text{ SD mm}^2/\text{s})$, with cut off 1.2×10^{-3} . Mature teratomas and endometriomas showed restricted diffusion with low ADC values (false positive).

Sensitivity of conventional MRI was 72.73% while that of DCE-MRI was 90.91%. The specificity was higher for DCE 100% compared to conventional MRI sequences 72.73%, as well as the accuracy which was 73.33% for conventional MRI while that of DCE was 96.67% and so addition of DCE to the MRI is expected to increase the specificity and the accuracy of examination.

Conclusion: Adding DWI and DCE to conventional MRI signifies: utilising a completely non-invasive procedure with no exposure to radiation. It enhances the specificity of MRI, hence enhancing the radiologist's confidence in image interpretation, which will ultimately affect the prognosis and outcome of patients.

Keywords: DW MRI; DCE MRI and ovarian masses.

1. INTRODUCTION

Cysts and tumours that are functional or benign are the most prevalent types of ovarian lesions [1].

Ovarian cancer is the most lethal of the gynecologic malignancies which is continuously challenging not only for physicians but radiologists as well [2].

“Ultrasound (US) is frequently the initial imaging examination conducted in the evaluation of a suspected ovarian lesion due to its wide availability, patient acceptability, non-invasiveness, and low cost” [3].

“In clinical routine, 5–25 % of adnexal lesions will remain indeterminate after sonography” [4].

Magnetic resonance imaging MRI performed after an ultrasound of an undetermined adnexal mass greatly improves the imaging evaluation's specificity, hence reducing the incidence of false-positive findings [5].

Due to its high spatial resolution and soft-tissue contrast, MRI has been shown to provide additional anatomical information about ovarian masses and nearby structures, which is beneficial for differentiating diagnoses [6,7].

Recently, diffusion-weighted imaging (DWI) has been included in gynecologic examinations [8].

“Diffusion-weighted imaging (DWI) has been increasingly used for qualitative and quantitative

tissue characterization in oncologic body imaging” [9].

“DCE-MRI relies on the leaking of contrast agent from capillaries into extravascular extracellular space, hence permitting quantitative analysis that represents blood flow and vascular permeability” [10].

Utilizing intravenous gadolinium enhances the detection of augmenting septa and solid mass components, as well as peritoneal and omental implants [11].

1.1 Aim of the Work

Evaluating the role of diffusion-weighted MR imaging in conjunction with dynamic contrast-enhanced MR imaging in the characterization of ovarian masses.

2. PATIENTS AND METHODS

This study comprised thirty female patients with ovarian masses of varying types. The majority of patients arrived with pelvi-abdominal pain and/or vaginal bleeding, and their ages ranged from 20 to 73.

Inclusion criteria:

- Female patient suspected to have a gynecological pelvic mass on clinical examination.
- Female patient done pelvic US examination diagnosing agynecological pelvic lesion.
- Female patient known to have previous ovarian tumor with surgical, radiotherapeutic or chemotherapeutic management.

Exclusion criteria: General contra-indications for MRI scan:

- Patients with metallic prosthesis; clips or devices in brain, eye & spinal canal. Patients with cardiac pacemakers, insulin pumps, neuro-stimulators & cochlear implants.
- Patients who had a history of claustrophobia.
- Patients with renal impairment

All the studied patients were subjected to the following:

- 1) **Complete history:** Full history was taken with a special emphasis on: Age, Time of menarche and Past history of gynecological troubles or operations.
- 2) **Laboratory investigations:** Including CBC, random blood sugar and kidney functions.
- 3) **Ultrasound examination:** Pelvi-abdominal and trans-vaginal.
- 4) **MRI examination:** MR imaging was performed by using GE Signa explorer 1.5-T MRI unit.

➤ **Patient preparation:** In order to reduce bowel peristalsis, 10 mg of an antispasmodic medication was administered intravenously before to MR imaging.

➤ **MR Imaging protocol:** The sequences used in the study (chart 1):

DW-MRI prior to contrast medium delivery, it was performed on all patients and acquired in the axial plane using a single shot echo-planar imaging sequence with b values (250, 500, 800 and 1000).

Dynamic contrast-enhanced MRI was done in all patients, post contrast gradient spine echo plane LAVA Flex images (on GE signa explorer 1.5 Tesla) were obtained immediately after manually injecting gadolinium at a dose of 0.1 mmol/kg of body weight (maximum, 20 mL), this was followed by injection of 20 mL of normal saline flushing the tube. Images were obtained sequentially to be consumed about 120 seconds in about 5 phases. Finally, axial, sagittal and coronal T1-weighted gradient-echo images were acquired.

Sequence	TR (msec.)	TE (msec.)	FOV(mm)	Slice thickness (mm)	Slice gap (mm)
T2 sagittal	4000-7000	110-120	FH=300mm RL=150mm AP=300mm	5	1
T2 Coronal	4000-7000	110-120	FH=300mm RL=300mm AP=150mm	5	1
T2 axial	4000-7000	110-120	FH=211mm AP=250mm RL=274mm	7	1.5
T1 axial	450-650	10-16	AP=250mm RL=274mm FH=211mm	7	1.5
DWI (4b-values:250, 500, 800,1000)	5000	70	38.0	7	1
LAVA Flex DCE-MRI on (gradient spine echo)	4.4	2.1	40	4	0
T1 Sagittal post contrast	450-650	10-16	AP=300mm RL=150mm FH=300mm	5	1
T1 coronal post contrast	450-650	10-16	AP=150mm RL=300mm FH=300mm	5	1
T1 axial post contrast	450-650	10-16	AP=250mm RL=274mm FH=211mm	7	1.5

MR Imaging analysis: MR images were analyzed for the following: • MR appearance of the tumor; whether cystic, solid or mixed, involvement of one or both ovaries, pre-contrast signal intensity of the included mass, enhancement of the solid component if present, wall thickness of the tumor and its enhancement, presence of vegetations, their enhancement pattern and their size, presence of ascites, presence of pathologically enlarged pelvic or para-aortic lymph nodes, soft tissue infiltration of other pelvic organs and presence of peritoneal or omental deposit.

2.1 Interpretation of DWI

Qualitative analysis: Regarding the signal intensity: we comment if the masses show low signal intensity on diffusion images with high signal in the corresponding ADC maps (facilitated) or show high signal intensity on diffusion images with lowering of the signal in the corresponding ADC maps (restricted).

Quantitative analysis: Regarding the quantitative analysis of DWI, we generated the ADC map and manually chose the ROI (region of interest) on the solid and cystic component of the tumours; the workstation then automatically calculated the ADC values. The ADC value was calculated for each mass lesion.

Interpretation of Dynamic contrast-enhanced MRI: Dynamic data were analyzed in consensus at a workstation. The entire adnexal mass is included in the five phases of dynamic run acquisition at 120 second after gadolinium injection. A region of interest (ROI) is manually drawn over the most avidly enhancing mass, solid component, thick enhanced wall or septations of the lesion. Signal intensity (SI)-time curve was performed.

There were three types of curve Type I curve showed steady rise with no definite peak, Type II curve showed moderate initial enhancement followed by a plateau and Type III curve showed initial rapid steep early enhancement and rapid wash out.

The maximum relative enhancement was automatically calculated by the computer software and was reported to know if it was more than 85% (with malignant) or less.

2.2 Statistical Analysis of the Data

Data were fed to the computer and analyzed using IBM SPSS software package version 20.0 (Armonk, NY: IBM Corp). Qualitative data were described using number and percent. The Kolmogorov-Smirnov test was used to verify the normality of distribution. Quantitative data were described using range (minimum and maximum), mean, standard deviation, Significance of the obtained results was judged at the 5% level. For comparing categorical data, Chi square test was performed. Agreement of the different predictives with the outcome was used and was expressed in sensitivity, specificity, positive predictive value, negative predictive value, and accuracy.

3. RESULTS

The patient's age ranged from 20 to 73 years (Mean age 40.37 ± 14.32 SD). The tumors pathologically were classified into 19 benign and 11 malignant tumors. Benign tumors included 5 dermoid cysts , 4 mucinous cystadenomas , 4 serous cystadenomas , 3 endometrioma , 3 simple cysts. Malignant tumors included 4 serous cystadenocarcinomas, 3 mucinous cystadenocarcinomas, 2 krukenberg tumors , one clear cell carcinoma and one endometrioid adenocarcinoma (Table 1).

Table 1. Histopathological types of studied cases (n= 30)

Tumor types	N	(%)
Benign		
Dermoid cyst	5	16.7
Endometrioma	3	10.0
Simple cyst	3	10.0
Mucinous cystadenoma	4	13.3
Serous cystadenoma	4	13.3
Malignant		
Serous cystadenocarcinoma	4	13.3
Clear cell carcinoma	1	3.3
Mucinous cystadenocarcinoma	3	10.0
Endometrioid adenocarcinoma	1	3.3
Krukenberg tumor	2	6.6

The tumors varied in their composition from being solid, cystic, mixed cystic and solid tumors. 13 cases showed typical criteria of malignant lesion by MRI. As complex cystic and solid lesions, presence of papillary projections and septations, presence of ascites, lesions of mixed SI and lesions of large size. Two cases suspected to be malignant by MRI according to size, presence of septae and solid nodule were proved to be benign by pathology (one serous cystadenoma, 1 mature teratoma) (Tables 2 and 3).

Nineteen cases showed restriction by DWI (high signal in diffusion images, low signal in corresponding ADC map and low ADC values ranging from 0.64 to 1.2 with average 0.91×10^{-3}), 11/19 proved to be malignant by pathology. 8/19 were false positive (5 mature teratomas and 3 endometriomas). Eleven cases showed facilitated diffusion (low signal in diffusion images, high signal on corresponding ADC map and high ADC values), all these cases proved to be benign pathologically (Tables 4,5 and 6).

Table 2. Distribution of the studied cases according to C MRI positive characters of malignancy (n = 30)

MRI positive characters of malignancy	No.	%
Malignant	13	43.3
Benign	17	56.7

Table 3. Agreement (sensitivity, specificity and accuracy) for C MRI (% from total)

Conventional MRI	Pathological result				Sensitivity	Specificity	PPV	NPV	Accuracy
	Benign (n =19)		Malignant (n=11)						
	No.	%	No.	%					
Benign	14	73.7	3	27.3	72.73	73.68	61.54	82.35	73.33
Malignant	5	26.3	8	72.7					

Table 4. Distribution of the studied cases according to DWI (n = 30)

	No.	%
Restricted diffusion (malignant criteria)		
No	11	36.7
Yes	19	63.3
low signal on the corresponding ADC map		
No	11	36.7
Yes	19	63.3
Low ADC values		
No	11	36.7
Yes	19	63.3

Table 5. Comparison of ADC values between benign and malignant ovarian masses (n = 30)

	Minimum	Maximum	Mean (\pm SD)
Benign masses(n=19)	0.81	3.0	1.68 \pm 0.65
Malignant masses (n=11)	0.64	1.20	0.91 \pm 0.25

Table 6. Agreement (sensitivity, specificity and accuracy) for DWI (% from total)

DWI MRI	Pathological result				Sensitivity	Specificity	PPV	NPV	Accuracy
	Benign (n =19)		Malignant (n=11)						
	No.	%	No.	%					
Benign	11	57.9	0	0.0	100.0	57.89	57.89	100.0	73.33
Malignant	8	42.1	11	100.0					

Ten cases showed tpe III curve with initial rapid steep early enhancement with MRE range from 100% to 180% with average 130% proved pathologically to be malignant. The nineteen true negative cases showed MRE range from 40% to 140% with average 73%. All of them showed tpe

I (slow rising) curve. One case showed type II curve with moderate initial enhancement followed by a plateau with MRE 110%, the pathology revealed malignant lesion (serous cystadeno carcinoma) (Tables 7,8 and 9).

Table 7. Distribution of the studied cases according to type of curves (n = 30)

Type of curves	No.	%
I	19	63.4
II	1	3.3
III	10	33.3

Table 8. Comparison between the maximum relative enhancement (MRE %) between benign and malignant tumors

MRE	Minimum	Maximum	Mean	Std. deviation
Benign	40	140	73	22.9
Malignant	100	180	130	27

Table 9. Agreement (sensitivity, specificity and accuracy) for DCE MRI (% from total)

DCE MRI	Pathological result				Sensitiv ity	Specific ity	PPV	NPV	Accura cy
	Benign (n =19)		Malignant (n=11)						
	No.	%	No.	%					
Benign and borderline	19	100.0	1	9.1	90.91	100.0	100.0	95.0	96.67
Malignant	0	0.0	10	90.9					

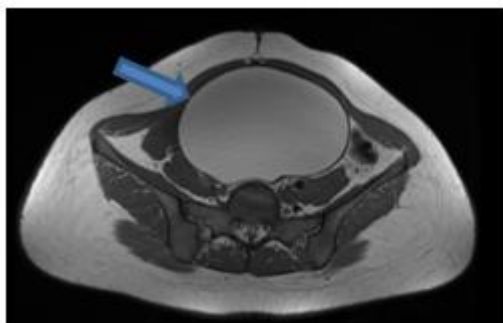


Fig. (a). Axial T1WI

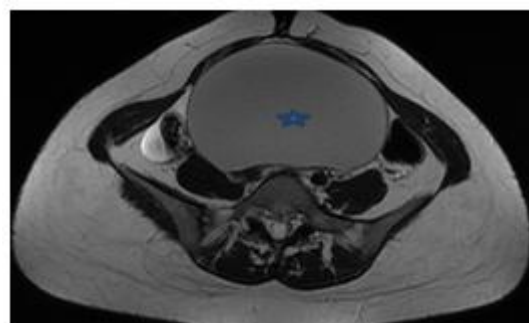


Fig. (b). Axial T2WI

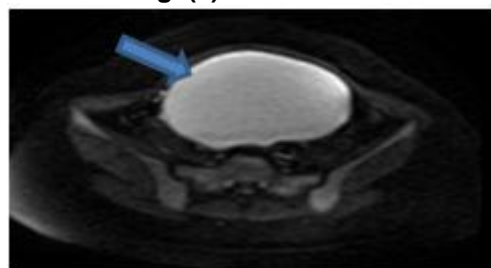


Fig. (c). DWI

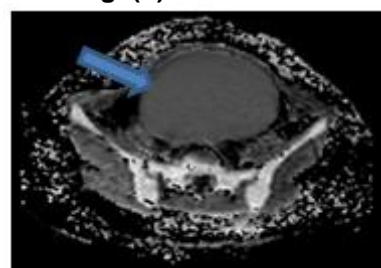


Fig. (d). ADC

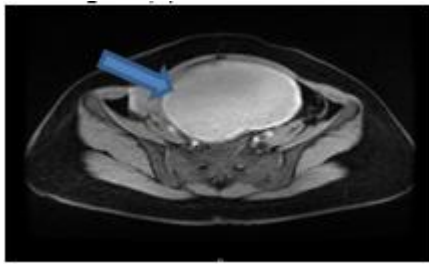


Fig. (e). Axial T1 post contrast

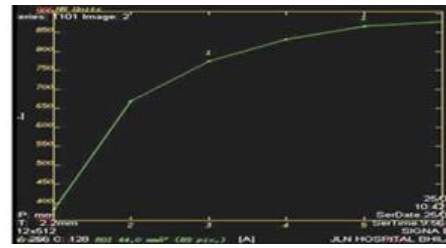


Fig. (f).Dynamic curve

Case 1: 25 years old female patient complaining of pelvic pain. Conventional MRI (a & b) showed a right ovarian cystic lesion measuring about 13.3x8.5x14.2 cm of homogenous high signal intensity (arrow)on T1 intermediate signal intensity on T2(astrisk) (T2 shading sign). DWI (c & d) showed restricted diffusion in the form of high signal on DWI with corresponding low signal on ADC map (arrowed). ADC value was $0.94 \times 10^{-3} \text{mm}^2/\text{s}$. DCE-MRI (e& f): the lesion showed faint wall enhancement (arrow) and the curve showed the criteria of benign lesion in the form of: slow rising curve (type 1), Pathological diagnosis was right ovarian endometrioma.

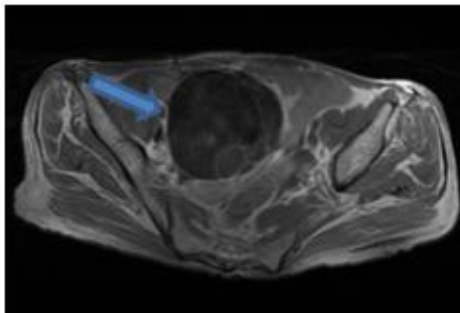


Fig. (a). Axial T1WI

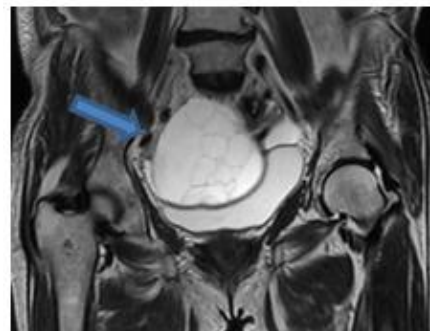


Fig. (b). Coronal T2WI

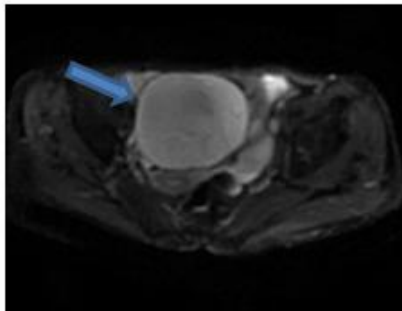


Fig. (c). DWI

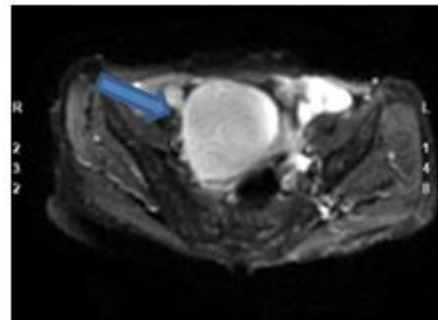


Fig. (d). ADC

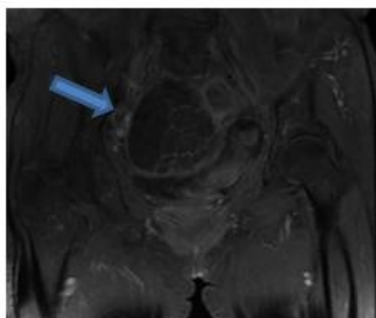


Fig. (d). Coronal post contrast fat suppressed T1WI

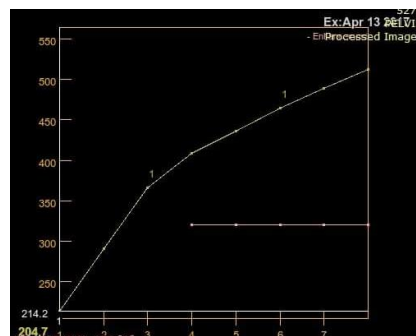


Fig. (f). Dynamic curve

Case 2: 27 years old female patient complaining of abdominal pain. Conventional MRI (a & b) showed right multi-locular adnexal cystic lesion measuring about 10x9 cm showing low T1 and high T2 signal intensity. DWI (c & d): showed facilitated diffusion in the form of low signal on DWI with corresponding high signal on ADC map

(arrowed). ADC value was $2 \times 10^{-3} \text{mm}^2/\text{s}$. DWI suggested benign nature. DCE-MRI (e & f): the lesion showed fine marginal (wall & septal) enhancement (arrowed) and type I curve (slow rising curve). Pathology revealed right ovarian mucinous cystadenoma.

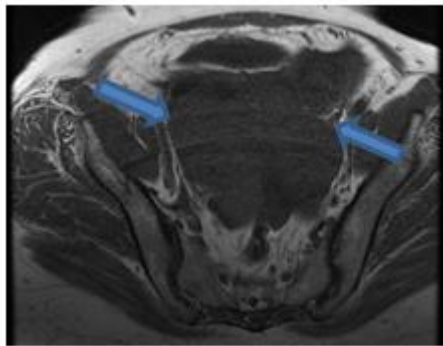


Fig. (a). Axial T1WI

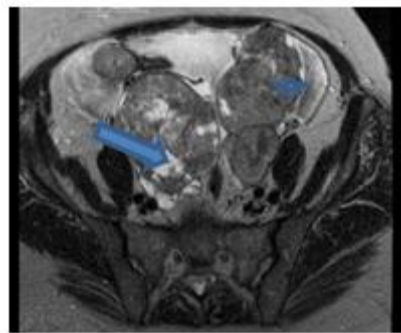


Fig. (b). Axial T2WI

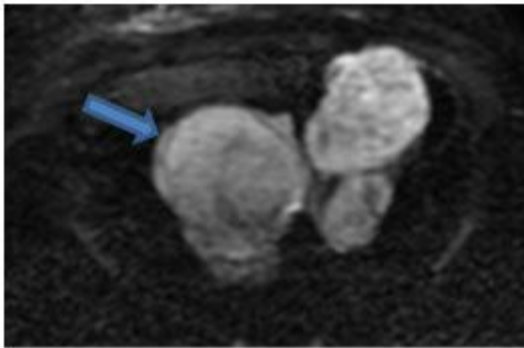


Fig. (c). DWI

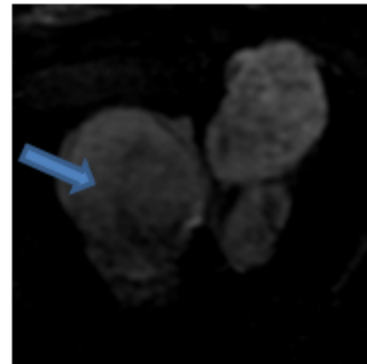


Fig. (d). ADC

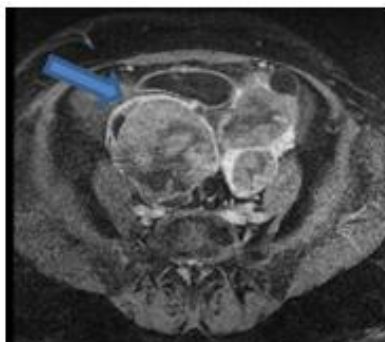


Fig. (e). Axial T1 post contrast

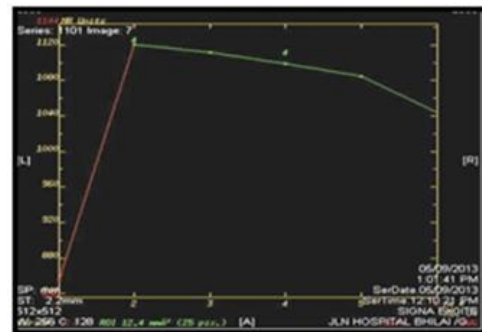


Fig. (f). Dynamic curve

Case 3: 39 years old female patient, known case of gastric cancer complaining of abdominal pain and vaginal bleeding. Conventional MRI (a & b) bilateral mixed cystic and solid adnexal mass lesions measuring about 10 x 5.5 x 12 cm on the right and 11.5 x 5 cm on the left of low signal intensity on T1 (arrowed), low signal of solid component (asterisk) with high signal intensity representing cystic degeneration on T2 (arrowed). DWI (c & d) showed restricted diffusion in the form of high signal on DWI with corresponding low signal on ADC map (arrowed). ADC value was $0.7 \times 10^{-3} \text{mm}^2/\text{s}$. DCE-MRI (e & f): the lesion showed heterogenous enhancement of the solid parts (arrow) and the curve showed the criteria of malignant lesion in the form of: rapid enhancement with rapid wash out curve (type III), Pathological diagnosis was bilateral Krukenberg tumor

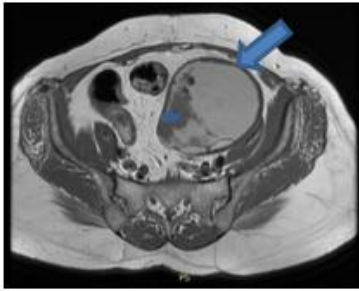


Fig. (a). Axial T1WI

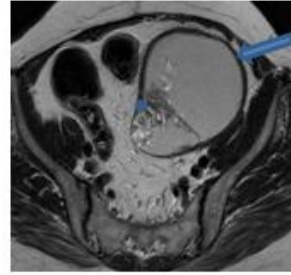


Fig. (b). Axial T2WI

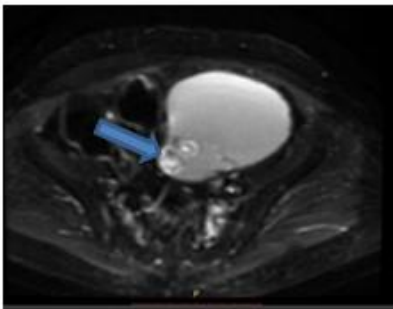


Fig. (c). DWI

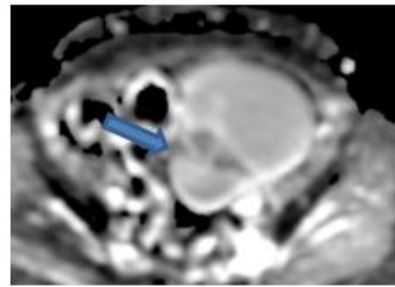


Fig. (d). ADC

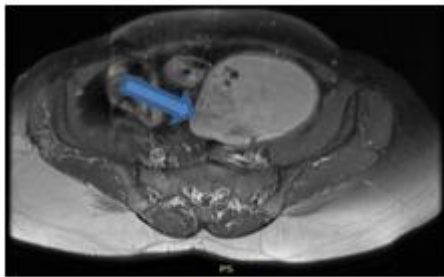


Fig. (e). Axial T1 post contrast

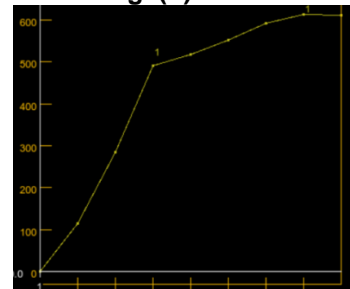


Fig. (f). Dynamic curve

Case 4: 56 years old female patient complaining of pelviabdominal pain not responding to medical treatment. Conventional MRI (a & b) left ovarian large complex cystic lesion with solid components measuring about 10.2 x10.3x11.5cm showing thick wall and septae with mural solid projections, showed high signal intensity for cystic components (arrow) and low signal intensity for solid components (asterisk) on T1, high signal intensity for cystic components (arrow) and mixed low and high signal intensity for solid components (asterisk) on T2. DWI (c & d) showed restricted diffusion in the form of high signal on DWI with corresponding low signal on ADC map (arrowed). ADC value was $0.79 \times 10^{-3} \text{mm}^2/\text{s}$. DCE-MRI (e & f): the lesion showed heterogeneous enhancement of the solid parts (arrow) and the curve showed the criteria of malignant lesion in the form of: rapid enhancement with rapid wash out curve (type III), Pathological diagnosis was clear cell carcinoma

4. DISCUSSION AND CONCLUSION

“Ovarian masses are a common finding in daily clinical practise and can be found or identified accidentally in symptomatic individuals. Characterization of an ovarian lesion is a diagnostic difficulty; it is crucial in the preoperative setting for planning appropriate therapeutic operations”. [10,11,9,7]. “With the use of a clinical examination, laboratory testing, and several imaging modalities, a complete preoperative evaluation is required for optimal management. Thus, aiding the patient in understanding the surgical route and the possibility of conservative treatment” [12,8].

MRI gives fine images of pelvic anatomy due to its high spatial resolution and tissue contrast; as a result, it plays a crucial role in the evaluation of ovarian lesions, distinguishing between benign and malignant lesions by finding distinguishing characteristics [12].

In our study, we included 30 patients with different ovarian lesions and we had performed an individual analysis for the pre-contrast MR sequences, DWI, and DCE-MR imaging regarding their diagnostic performance in differentiating between benign and malignant ovarian lesions.

In our study, we found that 72.7% of malignant cases are complex (cystic/solid) but only 26.3% of benign cases are complex, 100% of benign cases have no vegetations or papillary projections, mean width of malignant lesions (8.3 cm) is larger than in benign lesions (6.4 cm), 45.5 % of malignant cases show septations but only 26.3 % of benign cases show septations.

We agreed with Amir study carried on 84 patients that concluded both benign and malignant masses of the ovary can be distinguished on MRI according to texture whether cystic or solid, shape, size. The benign diagnosis on basis of cystic, no septations and vegetation on the wall while the malignant lesion has complex solid-cystic component, vegetation on the wall, large size of the lesion and presence of septations inside cystic adnexal lesion [13].

“DW-MRI is an important MR imaging technique which enables the radiologist to move from morphological to functional assessment of diseases of the female pelvis [14].

In this study, 63.3 % of the lesions showed restricted diffusion (hyper-intense signal in DWI and hypo-intense in ADC map), whereas 36.7% displayed facilitated diffusion (hypo-intense signal in DWI and hyper-intense in ADC map). We found that all the malignant (n=11, 100%) showed restricted diffusion with low ADC values”.

We agreed with Rajasri et al. study carried out “on 112 female patients with initial undetermined complex adnexal masses referred for MRI based on ultrasound findings for further characterization and staging, concluded that an adnexal mass with restricted diffusion usually is a malignant lesion, This finding, that of high signal intensity on DWI in solid components, may result from a reduction in both the extracellular matrix and the diffusion space of water protons in the extracellular and intracellular dimensions due to an increased nuclear to cytoplasmic ratio and hypercellularity” [15].

In our study, we had 19 pathologically proven benign ovarian lesions, 11 cases showed

facilitated diffusion and the rest 8 cases are (5 mature teratomas and 3 endometriomas) showed restricted diffusion, this was in agreement with Nasr et al. study which conducted on 30 cases of different ovarian lesions, twenty three cases were pathologically proved (classified to 12 benign and 11 malignant), seven cases showed facilitated diffusion (low signal in diffusion images, high signal on corresponding ADC map and high ADC values) and 5 endometriomas (proved pathologically) showed high signal on diffusion images [16].

Also, we agreed with Fujii and colleagues. Conducted a study “on 123 ovarian lesions, recorded that most malignant ovarian tumors, as well as some of the mature cystic teratomas, showed high signal intensity on DWI” [17].

In our study, we found that the mean ADC values for malignant lesions were $(0.91 \times 10^{-3} \pm 0.25 \text{ mm}^2/\text{s})$, while that for benign lesions were $(1.68 \times 10^{-3} \pm 0.65 \text{ mm}^2/\text{s})$ which was in agreement with Takeuchi and colleagues conducted on 47 women (33 malignant, 6 borderline, and 10 benign tumors). they concluded that the mean ADC value in malignant tumors $(1.03 \times 10^{-3} \pm 0.19 \text{ mm}^2/\text{s})$ was significantly lower than that in the 10 benign tumors $(1.38 \times 10^{-3} \pm 0.30 \text{ mm}^2/\text{s})$ [18].

In our study, we found that ADC value $\geq 1.2 \times 10^{-3} \text{ mm}^2/\text{s}$ may be the optimal cut off value for differentiating between benign and malignant tumors which was in agreement with Zhang et al. study carried on 191 female patients with different ovarian lesions underwent diffusion-weighted (DW) magnetic resonance (MR) imaging aiming to evaluate the role of DWI in differentiating between benign and malignant ovarian lesions, they concluded that ADC value $\geq 1.20 \times 10^{-3} \text{ mm}^2/\text{s}$ may be the optimal cutoff for differentiating between benign and malignant tumors [19].

In our study, the addition of the DWI improved the sensitivity and NPV of the conventional MRI from 72.73% and 82.35% to 100% and 100% respectively, yet the specificity was decreased from 73.68 % to 57.89 %; such low specificity elicited in our research is explained by the presence of benign cases that have mimicked malignancy on DWI; starting from their misleading signal intensities of restricted diffusion, down to the low ADC values measured such cases include teratomas and endometriomas.

A study done by Mansour S et al. found that "DWI is not an applicable way to discriminate benign from malignant ovarian masses. DWI can confirm or exclude potential malignancy in suspicious ovarian masses; provided (i) inclusion of the conventional MRI data, (ii) combined analysis of DWI quantitative and qualitative criteria and (iii) awareness of the sequence pitfalls. the sensitivity, specificity, PPV, NPV and accuracy of adding DWI to conventional MR imaging was 93.3%, 85 %, 88.5%, 94.4%, and 82.3% respectively compared to 93.3 %, 100 %, 100%,92.3%, and 95% after adding DCE-MRI to the conventional MR" [20].

DCE-MRI provides an accurate method for the prediction of malignancy, particularly in preoperative indeterminate cases [21].

In our work, 18 cases (60%) showed steady rise with no definite peak (type I curve), while 2 cases (6.7 %) showed moderate initial enhancement followed by a plateau (type II curve), and 10 cases(33.3 %) showed initial rapid steep early enhancement (type III curve). Sohaib and colleagues. described that "malignant lesion show greater enhancement than benign lesions during the early phase of enhancement rather than the late phase of enhancement while benign ovarian tumors showed a gradual increase in enhancement without a well-defined peak, while borderline ovarian tumors showed moderate initial enhancement followed by a plateau" [22].

In our work type III curve appeared specific for malignant tumors while type I curve was specific for benign tumors.

We agreed with Thomassin-Naggara and colleagues. showed that type III curve appeared specific for invasive tumors. Type I curve was more frequent in benign than in malignant tumors [8].

In this study, we found that Maximum relative enhancement ratio (MRE%) was significantly higher in malignant (mean value of $130\pm 27SD$) than in benign and borderline lesions (mean value $73\pm 22.9SD$). Also, there was some overlap regarding the MRE values between the benign and borderline lesions, however this can be used to exclude invasive malignancy.

We agreed with a study conducted by Mansour S et al. on 150 ovarian (42 benign, 26 borderline and 82 invasive malignant) masses evaluating the ability of dynamic post-contrast sequence to specify indeterminate ovarian masses with

inconclusive MR features of malignancy, showed that MRE % was higher for malignant than for benign and borderline masses [20].

In our study, the addition of the DCE MRI improved the sensitivity and specificity of the conventional MRI from 72.73% and 73.68 to 90.91% and 100% respectively.

This agrees with a study conducted by Li and colleagues. "differentiating malignant and benign ovarian lesions on 48 ovarian tumors (13 benign and 35 malignant) investigated produced a sensitivity of 100% and specificity of 92.31%" [23].

ETHICAL APPROVAL

The Research Ethical Committee of the Faculty of Medicine of Tanta University approved the project.

CONSENT

As per international standard or university standard, patients' written consent has been collected and preserved by the author(s).

COMPETING INTERESTS

Authors have declared that no competing interests exist.

REFERENCES

1. Patrick UE and Lucky Kbenign ovarian tumours in a tertiary care hospital in Niger Delta, Nigeria: A 10 year histopathological study. *International Journal of Current Research and Review*. 2015;7(8):71.
2. Lu KH, Skates S, Hernandez MA, Bedi D, Bevers T, Leeds L, et al. A 2-stage ovarian cancer screening strategy using the Risk of Ovarian Cancer Algorithm (ROCA) identifies early-stage incident cancers and demonstrates high positive predictive value. *Cancer*. 2013;119(19):3454-61.
3. Jeong Y-Y, Outwater EK and Kang HK. Imaging evaluation of ovarian masses. *Radiographics*. 2000;20(5):1445-70.
4. Van Calster B, Timmerman D, Valentin L, McIndoe A, Ghaem-Maghani S, Testa AC, et al. Triaging women with ovarian masses for surgery: observational diagnostic study to compare RCOG guidelines with an International Ovarian Tumour Analysis

- (IOTA) group protocol. *Bjog*. 2012; 119(6):662-71.
5. Anthoulakis C and Nikoloudis N. Pelvic MRI as the "gold standard" in the subsequent evaluation of ultrasound-indeterminate adnexal lesions: a systematic review. *Gynecol Oncol*. 2014;132(3):661-8.
 6. Mohaghegh P and Rockall AG. Imaging strategy for early ovarian cancer: characterization of adnexal masses with conventional and advanced imaging techniques. *Radiographics*. 2012;32(6):1751-73.
 7. Foti PV, Attinà G, Spadola S, Caltabiano R, Farina R, Palmucci S, et al. MR imaging of ovarian masses: classification and differential diagnosis. *Insights into imaging*. 2016;7(1):21-41.
 8. Thomassin-Naggara I, Toussaint I, Perrot N, Rouzier R, Cuenod CA, Bazot M, et al. Characterization of complex adnexal masses: value of adding perfusion- and diffusion-weighted MR imaging to conventional MR imaging. *Radiology*. 2011;258(3):793-803.
 9. Harry VN. Novel imaging techniques as response biomarkers in cervical cancer. *Gynecol Oncol*. 2010;116(2):253-61.
 10. Andrew N, Andrew B, Masako K, et al. Dynamic contrast enhanced MRI in ovarian cancer: Initial experience in 3 Tesla in primary and metastatic disease. *Magn Reson Med* 2010;63: 1044-104.
 11. Iyer VR and Lee SI. MRI, CT, and PET/CT for ovarian cancer detection and adnexal lesion characterization. *Am J Roentgenol*. 2010;194(2):311-21.
 12. Vargas HA, Barrett T and Sala E. MRI of ovarian masses. *J Magn Reson Imaging*. 2013;37(2):265-81.
 13. Amir K. Validity of Magnetic Resonance Imaging (MRI) in characterizing adnexal masses: a prospective study: *Journal of Chemical and Pharmaceutical Sciences* 2017;10(1):142-146.
 14. Sala E, Rockall A, Rangarajan D and Kubik-Huch RA. The role of dynamic contrast-enhanced and diffusion weighted magnetic resonance imaging in the female pelvis. *Eur J Radiol*. 2010;76(3):367-85.
 15. Rajasri B. , Prasad H. and Sree S. Role of Diffusion Weighted MR Imaging in Adnexal lesions in Female Pelvis A Prospective study: *JMSCR* 2016;4(9): 12675-12685.
 16. Nasr E, Hamed I, Abbas I and Khalifa NM. Dynamic contrast enhanced MRI in correlation with diffusion weighted (DWI) MR for characterization of ovarian masses. *Egypt J Radiol Nucl Med*. 2014;45(3):975-85.
 17. Fujii S, Kakite S, Nishihara K, Kanasaki Y, Harada T, Kigawa J, et al. Diagnostic accuracy of diffusion-weighted imaging in differentiating benign from malignant ovarian lesions. *J Magn Reson Imaging*. 2008;28(5):1149-56.
 18. Takeuchi M, Matsuzaki K and Nishitani H. Diffusion-weighted magnetic resonance imaging of ovarian tumors: differentiation of benign and malignant solid components of ovarian masses. *J Comput Assist Tomogr*. 2010;34(2):173-6.
 19. Zhang P, Li W, Chu C, Cui Y and Zhu M. Diffusion-weighted MRI: a useful technique to discriminate benign versus malignant ovarian surface epithelial tumors with solid and cystic components 2012; 37: 897-903.
 20. Mansour S, Saraya S and El-Faissal Y. Semi-quantitative contrast-enhanced MR analysis of indeterminate ovarian tumours: when to say malignancy? *Br J Radiol*. 2015;88(1053):20150099.
 21. Dogheim OY, Hamid AE-DMA, Barakat MS, Eid M and El-Sayed SM. Role of novel magnetic resonance imaging sequences in characterization of ovarian masses. *The Egyptian Journal of Radiology and Nuclear Medicine*. 2014;45(1):237-51.
 22. Sohaib SA, Sahdev A, Trappen PV, Jacobs IJ and Reznek RH. Characterization of adnexal mass lesions on MR imaging. *Am J Roentgenol*. 2003;180(5):1297-304.
 23. Li H-M, Qiang J-W, Ma F-H and Zhao S-H. The value of dynamic contrast-enhanced MRI in characterizing complex ovarian tumors. *J Ovarian Res*. 2017;10(1):4.

© 2022 Radwan et al.; This is an Open Access article distributed under the terms of the Creative Commons Attribution License (<http://creativecommons.org/licenses/by/4.0>), which permits unrestricted use, distribution, and reproduction in any medium, provided the original work is properly cited.

Peer-review history:

The peer review history for this paper can be accessed here:

<https://www.sdiarticle5.com/review-history/84922>